

# Meson formfactor scheme for the chiral Lagrangian approach to $J/\psi$ breakup cross sections motivated by a relativistic quark model

D. B. Blaschke

*Institute for Theoretical Physics, University of Wrocław, 50-204 Wrocław, Poland and*

*Bogoliubov Laboratory for Theoretical Physics,*

*JINR Dubna, 141980 Dubna, Russia*

H. Grigorian and Yu. L. Kalinovsky

*Laboratory of Information Technologies,*

*JINR Dubna, 141980 Dubna, Russia*

(Dated: July 4, 2009)

## Abstract

We suggest a new scheme for the introduction of formfactors for the  $SU(4)$  chiral meson Lagrangian approach to the  $J/\psi$  breakup cross sections by pion and rho meson impact. This mesonic formfactor scheme respects the fact that on the quark level of description the contact and the meson exchange diagrams are constructed by so-called box and triangle diagrams which contain a different number of vertex functions for the quark-meson coupling. We present a model calculation for Gaussian vertex functions within the meson formfactor scheme and compare the results with those of the usual global formfactor model. We calibrate the new meson formfactor model with results for the pion impact processes from a relativistic quark model calculation by Ivanov et al. and present predictions for the  $\rho$ -meson induced processes. We provide a fit formula for the resulting energy-dependent cross sections.

## I. INTRODUCTION

The  $J/\psi$  meson plays a key role in the experimental search for the quark-gluon plasma (QGP) in heavy-ion collision experiments where an anomalous suppression of its production cross section relative to the Drell-Yan continuum as a function of the centrality of the collision has been found by the CERN-NA50 collaboration [1]. An effect like this has been predicted to signal QGP formation [2] as a consequence of the screening of color charges in a plasma in close analogy to the Mott effect (metal-insulator transition) in dense electronic systems [3]. However, a necessary condition to explain  $J/\psi$  suppression in the static screening model is that a sufficiently large fraction of  $c\bar{c}$  pairs after their creation have to traverse regions of QGP where the temperature (resp. parton density) has to exceed the Mott temperature  $T_{J/\psi}^{\text{Mott}} \sim 1.2 - 1.3 T_c$  [4, 5] for a sufficiently long time interval  $\tau > \tau_f$ , where  $T_c \sim 190$  MeV is the critical phase transition temperature and  $\tau_f \sim 0.3$  fm/c is the  $J/\psi$  formation time. Within an alternative scenario [6],  $J/\psi$  suppression does not require temperatures well above the deconfinement one but can occur already at  $T_c$  due to impact collisions by quarks from the thermal medium. An important ingredient for this scenario is the lowering of the reaction threshold for string-flip processes which lead to open-charm meson formation and thus to  $J/\psi$  suppression. This process has an analogue in the hadronic world, where e.g.  $J/\psi + \pi \rightarrow D^* + \bar{D} + h.c.$  could occur provided the reaction threshold of  $\Delta E \sim 640$  MeV can be overcome by pion impact. It has been shown [7, 8] that this process and its in-medium modification can play a key role in the understanding of anomalous  $J/\psi$  suppression as a deconfinement signal. Since at the deconfinement transition the  $D$ -mesons enter the continuum of unbound (but strongly correlated) quark-antiquark states (Mott-effect), their spectral function is broadened and the relevant threshold for charmonium breakup is effectively lowered so that the reaction rate for the process gets critically enhanced [9]. Thus a process which is almost negligible in the vacuum may give rise to additional (and therefore anomalous)  $J/\psi$  suppression when conditions of the chiral/ deconfinement transition and  $D$ -meson Mott effect are reached in a heavy-ion collision. The dissociation of the  $J/\psi$  itself still needs impact to overcome the threshold which is still present but dramatically reduced.

For this alternative scenario [7] to work the  $J/\psi$  breakup cross section by meson impact is required and its dependence on the masses of the final state  $D$ -mesons has to be determined.

After the first calculations of this quantity within a nonrelativistic potential model (NPM) [10] and its systematic improvement [11], the relativistic quark model (RQM) calculation suggested in [12] could recently be completed for  $J/\psi$  dissociation processes by pion impact [13]. Both approaches result in energy dependent cross sections with a steep rise to a maximum of the order of 1 mb close to the threshold followed by a fast drop. This agreement in shape and magnitude is a nontrivial result since the NPM contains quark and gluon exchange diagrams only at first Born order whereas the RQM includes meson exchange diagrams between the colliding mesons, which correspond to ladder-type resummation of gluon exchanges.

Shortly after the publication of the NPM results, a chiral Lagrangian (CL) approach to the problem of  $J/\psi$  dissociation has been suggested [14] which resulted in qualitatively different predictions for the magnitude and the energy dependence of the dissociation cross sections: a monotonously rising behaviour which reached the level of 1 mb only about 400 MeV above the threshold. In this work, however, important processes have not been considered and subsequent, more systematic developments of the CL approach [15, 16, 17, 18, 19, 20] have revealed the importance of  $D^*$  meson exchange and contact diagrams. Their inclusion lead to a steep rise of the cross section at the threshold to a level of several tens of millibarns followed by a continuous rise with increasing energy. It has been admitted, however, that this monotonously rising behaviour of the cross section is an artifact of the treatment of mesons as pointlike particles in the CL approach. Phenomenological formfactors have therefore been introduced in order to take into account the finite size of meson-meson vertices due to the composite nature of the mesons. Unfortunately, the results of the formfactor-improved CL models (FCLM) appear to be strongly dependent on the choice of those formfactors for the meson-meson vertices [15, 18, 19, 21, 22, 23]. This is a basic flaw of these approaches which could only be overcome when a more fundamental approach, e.g., from a quark model, can determine these input quantities of the chiral Lagrangian approach. There have been attempts to reduce the uncertainties of the FCLM by constraining the choice of the formfactor using a comparison with results of the NPM approach which makes use of meson wave functions [21, 22].

In the present work we suggest a formfactor model which takes into account the different sizes of mesons in the collision by meson-dependent range parameters and accounts for the fact that in a RQM the contact diagrams are represented by a quark loop containing four

mesonic wave functions (box diagram) which suppress the transition amplitude at high momentum transfer, while meson exchange diagrams are represented by the product of triangle diagrams containing six meson wave functions. We calibrate the parameters of this meson formfactor model by comparison with a RQM calculation of the  $J/\psi$  dissociation by pion impact [13]. On the basis of this newly developed meson formfactor CL (MFCL) model we make a prediction for the rho-meson impact dissociation processes of the  $J/\psi$  meson. We suggest that this MFCL model can be applied for the calculation of the in-medium modification of the  $J/\psi$  breakup due to the Mott-effect for mesonic states at the deconfinement/chiral restoration transition according to the quantum kinetic approach suggested in [7, 8] and provide an explanation of the anomalous  $J/\psi$  suppression effect observed in heavy-ion collisions at the CERN-SPS [1]. The MFCL approach developed here can be applied also to  $J/\psi$  dissociation by nucleon impact which is of central importance for the quark matter diagnostics under dense nuclear matter conditions as, e.g., in the planned CBM experiment at FAIR Darmstadt or at NICA Dubna.

## II. $J/\psi$ BREAKUP CROSS SECTIONS FOR $\pi$ AND $\rho$ MESON IMPACT FROM THE CHIRAL LAGRANGIAN APPROACH

The effective Lagrangian approach we employ in the present study is developed in Ref. [17] based on the minimal  $SU(4)$  Yang-Mills Lagrangian including anomalous parity interactions which are connected to the gauged Wess-Zumino action, namely  $\pi + J/\psi \rightarrow D + \bar{D}$ ,  $\pi + J/\psi \rightarrow D^* + \bar{D}^*$  and  $\rho + J/\psi \rightarrow D^* + \bar{D}$ . The processes we discuss in the following on this basis are thus

$$J/\psi + \pi \rightarrow D + \bar{D}, D^* + \bar{D}, D + \bar{D}^*, D^* + \bar{D}^* \quad (1)$$

$$J/\psi + \rho \rightarrow D + \bar{D}, D^* + \bar{D}, D + \bar{D}^*, D^* + \bar{D}^*. \quad (2)$$

The corresponding cross sections after averaging (summing) over initial (final) spins and including isospin factors can be represented in a form given by

$$\frac{d\sigma}{dt} = \frac{1}{64\pi s p_{cm}^2 I_s I_i} M_{\lambda_k \dots \lambda_l} M_{*\lambda'_k \dots \lambda'_l} N_k^{\lambda_k \lambda'_k}(p_k) \dots N_l^{\lambda_l \lambda'_l}(p_l) , \quad (3)$$

where the  $s, t, u$  are the standard Mandelstam variables,

$$p_{cm}^2 = \frac{[s - (m_1 + m_2)^2][s - (m_1 - m_2)^2]}{4s} \quad (4)$$

is the squared momentum of initial state mesons in the center-of-momentum frame. In Eq. (3) we have introduced the projectors

$$N_k^{\lambda\lambda'}(q) = \left( g^{\lambda\lambda'} - \frac{q^\lambda q^{\lambda'}}{m_k^2} \right) = \varepsilon^\lambda(q) \cdot \varepsilon^{*\lambda'}(q) \quad (5)$$

corresponding to each involved vector particle of species  $k$  and their relationship to the polarisation vectors  $\varepsilon^\lambda(q)$  employed, e.g., in Ref. [17]. This notation makes explicit that each amplitude contributing to the differential cross section (3) is manifestly gauge invariant  $p^{\lambda_k} M_{\lambda_k \dots \lambda_l} = 0$ . The factors  $I_s$  and  $I_i$  result from averaging over initial spins and isospins, respectively. Their evaluation amounts to  $I_s I_i = 3/2$  for the processes in Eq. (1) and to  $I_s I_i = 9/2$  for those in Eq. (2). The amplitudes  $M_{\lambda_k \dots \lambda_l} = \sum_{j=1}^s M_{\lambda_k \dots \lambda_l}^{(j)}$  of the corresponding processes are collected in tables given in the Appendix. The index  $j$  specifies the diagram which contributes to a process with given initial and final states. In the tables we use the  $Q$  for the momentum of the exchanged  $D$  and  $D^*$  mesons. For  $t$ -channel exchange we have  $Q = p_1 - p_3$  while for  $u$ -channel exchange  $Q = p_2 - p_3$  holds. The results for the energy dependent cross sections of the  $J/\psi$  breakup processes by pion and rho-meson impact are shown in Fig. 1. The unknown coupling constants of the chiral Lagrangian approach are fixed according to the scheme given in Ref. [17] which is based on the  $SU(4)$  symmetry relations, the vector dominance model and the observed decay  $D^* \rightarrow D\pi$ . The resulting values of [17] are given in the Table of Appendix B.

As it has been discussed in the Introduction, the monotonous rise of the cross section with increasing energy has to be considered as an unphysical artifact of the neglect of the finite size of the mesons due to their quark substructure. In the following Section we suggest a new scheme for introducing hadronic formfactors which is based on the insight from the NPM (RQM) that they originate from the meson wavefunctions (Bethe-Salpeter amplitudes) involved in the representation of the meson vertices by quark exchange (quark loop) diagrams.

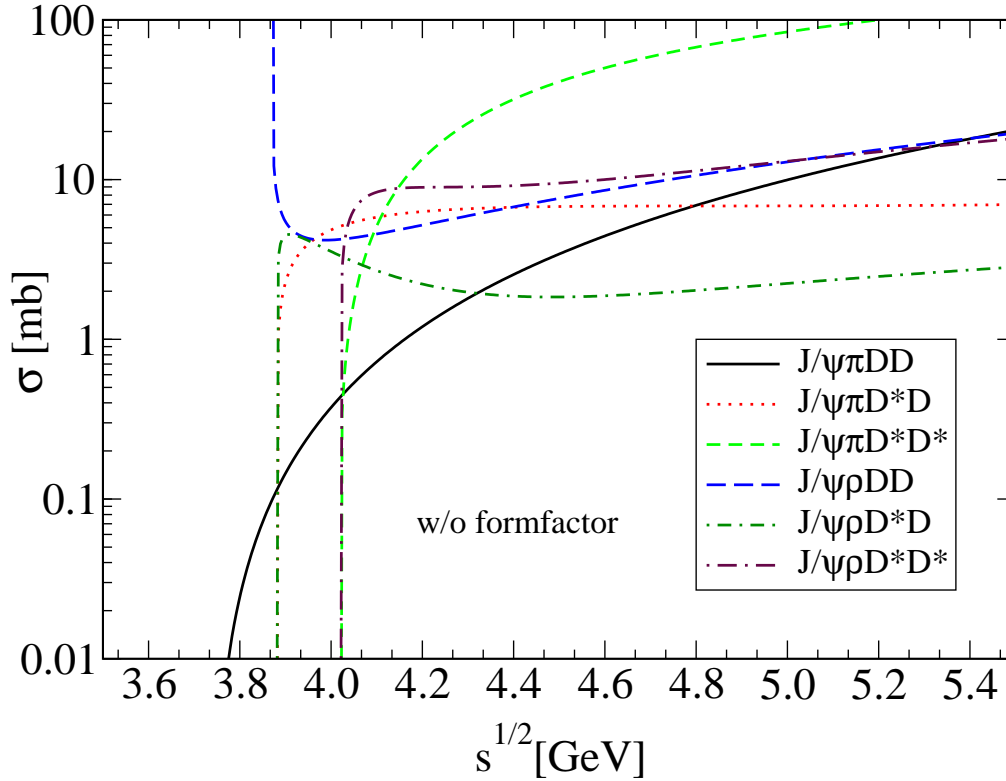


FIG. 1: (Color online)  $J/\psi$  break-up cross sections by pion and rho-meson impact in the chiral Lagrangian model without formfactors.

### III. HADRONIC FORMFACTORS

The chiral Lagrangian approach for  $J/\psi$  breakup by light meson impact makes the assumption that mesons and meson-meson interaction vertices are pointlike (four-momentum independent) objects. This neglect of the finite extension of mesons as quark-antiquark bound states has dramatic consequences: it leads to a monotonously rising behaviour of the cross sections for the corresponding processes, see Fig. 1.

This result, however, cannot be correct away from the reaction threshold where the tails of the mesonic wave functions determine the high-energy behaviour of the quark exchange (in the nonrelativistic formulation of [10, 11]) or quark loop (in the relativistic formulation [12, 13]) diagrams describing the microscopic processes underlying the  $J/\psi$  breakup by meson impact. Since the mesonic wave functions describing quark-antiquark bound states have a finite extension in coordinate- and momentum space, the  $J/\psi$  breakup cross sec-

tion is expected to be decreasing function for high c.m. energies of the collision. Such a behaviour has been obtained within NPM and RQM approaches to meson-meson interactions [10, 11, 12, 13]. In order to model such a behaviour within chiral meson Lagrangian approaches one uses formfactors at the interaction vertices [15, 19, 21, 22] which can be calibrated using quark model results for available processes. On this basis the cross sections for otherwise unknown processes can be predicted. When the amplitudes of all subprocesses are separately gauge invariant (see the discussion of Eqs. (3) and (5) in Sect. II), the procedure of their rescaling with different three-momentum dependent formfactors does not violate the gauge invariance of the chiral Lagrangian approach. However, the violation of the transversality requirement by assuming different formfactors for processes (which are not separately transversal as motivated for example by the relativistic quark model) should not be mismatched with a possible violation of the conservation laws by the considered processes. Due to the implementation of phenomenological formfactors our approach qualifies as an effective one for which conservation laws are fulfilled by the construction of the amplitudes for interaction vertices.

### A. Global formfactor ansatz

The simplest ansatz for a hadronic formfactor disregards the specifics of different mesonic species such as the different radii of their wave functions. Following the definitions of Ref. [15], the formfactor of all the four-meson vertices given in the Appendix A, i.e. those of the contact diagrams as well as those of the meson exchange diagrams is given in the same form. It is represented as a product of the three-meson vertices and intermediate meson propagation

$$F_4(\mathbf{q}^2) = \left[ F_3(\mathbf{q}^2) \right]^2 . \quad (6)$$

In this formula,  $\mathbf{q}^2$  is given by the average value of the squared three-momentum transfers in the  $t$  and  $u$  channels

$$\mathbf{q}^2 = \frac{1}{2} \left[ (\mathbf{p}_1 - \mathbf{p}_3)^2 + (\mathbf{p}_2 - \mathbf{p}_3)^2 \right]_{\text{c.m.}} = p_{i,\text{c.m.}}^2 + p_{f,\text{c.m.}}^2 . \quad (7)$$

Here,  $p_{i,\text{c.m.}}$  and  $p_{f,\text{c.m.}}$  can be represented by using the Mandelstam variables  $s$

$$\begin{aligned} p_{i,\text{c.m.}}^2 &= \frac{1}{4s} \left( s - (m_1 + m_2)^2 \right) \left( s - (m_1 - m_2)^2 \right), \\ p_{f,\text{c.m.}}^2 &= \frac{1}{4s} \left( s - (m_3 + m_4)^2 \right) \left( s - (m_3 - m_4)^2 \right). \end{aligned} \quad (8)$$

For the three-meson vertices, we use formfactors with a momentum dependence in the Gaussian ( $G$ ) form

$$F_3(\mathbf{q}^2) = \exp(-\mathbf{q}^2/\Lambda^2) , \quad (9)$$

motivated by the behavior of a mesonic bound state wave function. The results for the  $J/\psi$  breakup cross sections by light meson impact with this global formfactor model are shown in Fig. 2.

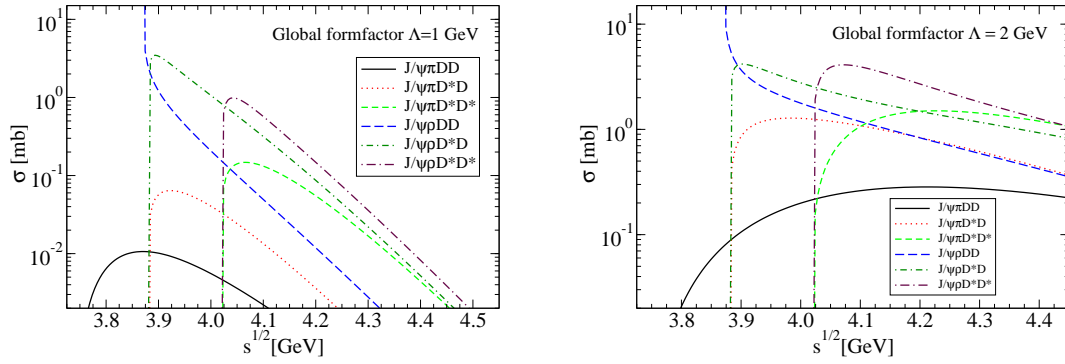


FIG. 2: (Color online)  $J/\psi$  break-up cross sections in the chiral Lagrangian model with Gaussian global formfactors and range parameters  $\Lambda = 2$  GeV (left panel) and  $\Lambda = 1$  GeV (right panel).

## B. Meson formfactor ansatz

In order to take into account the quark substructure of meson-meson vertices we suggest here a simple ansatz which respects the different sizes of the interacting mesons and the different quark diagram representations in terms of quark box and quark triangle diagrams. The triangle diagram is of third order in the wave functions so that the meson exchange diagrams are suppressed at large momentum transfer by six wave functions while the box diagram appears already at fourth order thus being less suppressed than suggested by the ansatz (6) of Ref. [15].

For the contact terms (four-meson vertices) we introduce according to the scheme  $g_{J/\psi\pi D^*D} \longrightarrow g_{J/\psi\pi D^*D} \times F_c(s)$  the contact formfactors  $F_c(s)$  in the following form

$$F_c(s) = \exp \left\{ - \left[ p_{i,\text{c.m.}}^2 \left( \frac{1}{\Lambda_1^2} + \frac{1}{\Lambda_4^2} \right) + p_{f,\text{c.m.}}^2 \left( \frac{1}{\Lambda_3^2} + \frac{1}{\Lambda_2^2} \right) \right] \right\} \quad (10)$$

The formfactors  $F_u(s, t)$  for the  $u$ - channel meson exchange terms are introduced according to the example  $g_{J/\psi D^* D^*} \times g_{D^* D \pi} \longrightarrow g_{J/\psi D^* D^*} \times g_{D^* D \pi} \times F_u(s, t)$  with the form

$$F_u(s, t) = \exp \left\{ - \left[ p_{i,\text{c.m.}}^2 \left( \frac{1}{\Lambda_1^2} + \frac{1}{\Lambda_4^2} \right) + p_{f,\text{c.m.}}^2 \left( \frac{1}{\Lambda_3^2} + \frac{1}{\Lambda_4^2} \right) + \frac{2\mathbf{q}(s, t)^2}{\Lambda_4^2} \right] \right\}. \quad (11)$$

Analogously, the formfactor  $F_t(s)$  for the  $t$ - channel meson exchange diagrams is introduced according to the example  $g_{J/\psi DD} \times g_{D^* D \pi} \longrightarrow g_{J/\psi DD} \times g_{D^* D \pi} \times F_t(s, u)$  with the formfactor

$$F_t(s, u) = \exp \left\{ - \left[ p_{i,\text{c.m.}}^2 \left( \frac{1}{\Lambda_1^2} + \frac{1}{\Lambda_2^2} \right) + p_{f,\text{c.m.}}^2 \left( \frac{1}{\Lambda_3^2} + \frac{1}{\Lambda_4^2} \right) + \frac{2\mathbf{q}(s, u)^2}{\Lambda_3^2} \right] \right\} \quad (12)$$

and is related to the  $F_u(s, t)$  by exchanging  $u \leftrightarrow t$  and  $\Lambda_3 \leftrightarrow \Lambda_4$ . Here the  $\mathbf{q}^2(s, t)$  can be also rewritten using the Mandelstam variables  $s, t$  and  $u$  as

$$\mathbf{q}^2(s, t) = \left( (m_1^2 - m_2^2) - (m_3^2 - m_4^2) \right)^2 / 4s - t; \quad (13)$$

for the  $t$ -channel and

$$\mathbf{q}^2(s, u) = \left( (m_1^2 - m_2^2) + (m_3^2 - m_4^2) \right)^2 / 4s - u; \quad (14)$$

for the  $u$ -channel meson exchange processes. The dependences of the formfactors on  $p_{i,\text{c.m.}}^2, p_{f,\text{c.m.}}^2$  on the transferred momentum  $\mathbf{q}$  are the same as in the global formfactor case, see Eq.(8). Here we use the phenomenological range parameters  $\Lambda_i = \alpha \Lambda_i^0$  of the meson-quark-antiquark vertices which shall resemble the ranges of the corresponding meson wave functions in momentum space and thus be closely related to the meson masses  $m_i$ , see Table I. The physical meaning of such an approach is to take into account that for high energies the cross-section of given process is suppressed due to the lack of time for quark exchange between interacting mesons as well as due to the reduction of the overlap of meson wave functions. The ansatz of the effective range according to the rule  $\left( 1/\Lambda_1^2 + 1/\Lambda_2^2 \right)$  means that in the case of different meson sizes the amount of suppression is dominated by heavier, i.e. the smaller meson. Such an ansatz is in accord with the phenomenological Povh-Hüfner law for total hadron-hadron cross sections [24]. For later use, we introduce additionally a common scale factor  $\alpha$  to be used in fixing the formfactor by comparison with the RQM approach of Ref. [13].

state $i$	$J/\psi$	$D^*$	$D$	$\varrho$	$\pi$
$m_i[\text{GeV}]$	3.1	2.01	1.87	0.77	0.14
$\Lambda_i^0[\text{GeV}]$	3.1	2.0	1.9	0.8	0.6

TABLE I: (Color online) Meson masses and range parameters corresponding to the quark-antiquark-meson vertices as used in the meson formfactor ansatz of Subsection III B.

The results are depicted in Figs. 3 and 4. In the last Section, we discuss the results and their possible implications for phenomenological applications.

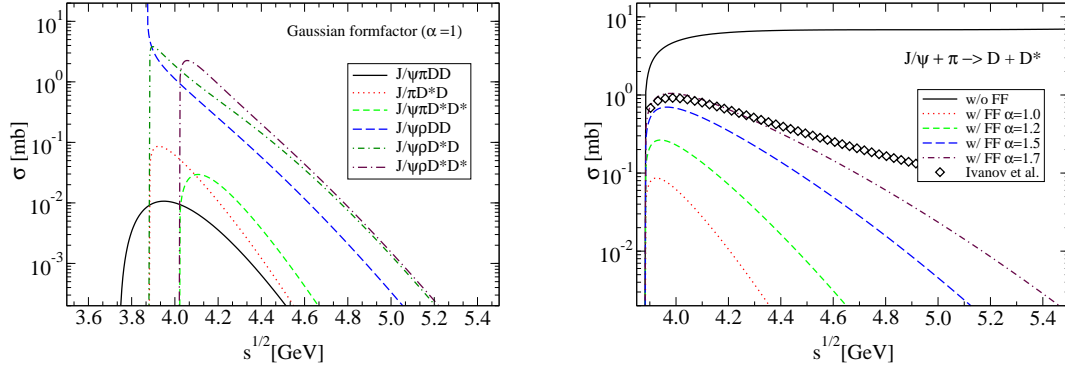


FIG. 3: (Color online) Left panel:  $J/\psi$  break-up cross sections in the chiral Lagrangian model with Gaussian mesonic formfactors and scale factor  $\alpha = 1$ . Right panel: Dependence of the cross section for the process  $J/\psi + \pi \rightarrow D + D^*$  on the scale parameter  $\alpha$  in the mesonic formfactors. For  $\alpha = 1.7$  one reproduces the results of the RQM calculation [13].

#### IV. RESULTS

The  $J/\psi$  breakup cross sections by  $\pi$  and  $\rho$  meson impact have been formulated within a chiral  $SU(4)$  Lagrangian approach including anomalous processes. The use of formfactors at the meson-meson vertices is mandatory since otherwise the high-energy asymptotics of the processes with hadronic final states will be overestimated as shown in Fig. 1. From a comparison of the results for the global formfactor ansatz with a Gaussian function using range parameters  $\Lambda = 1$  GeV and  $\Lambda = 2$  GeV in Fig. 2 we show that the difference in

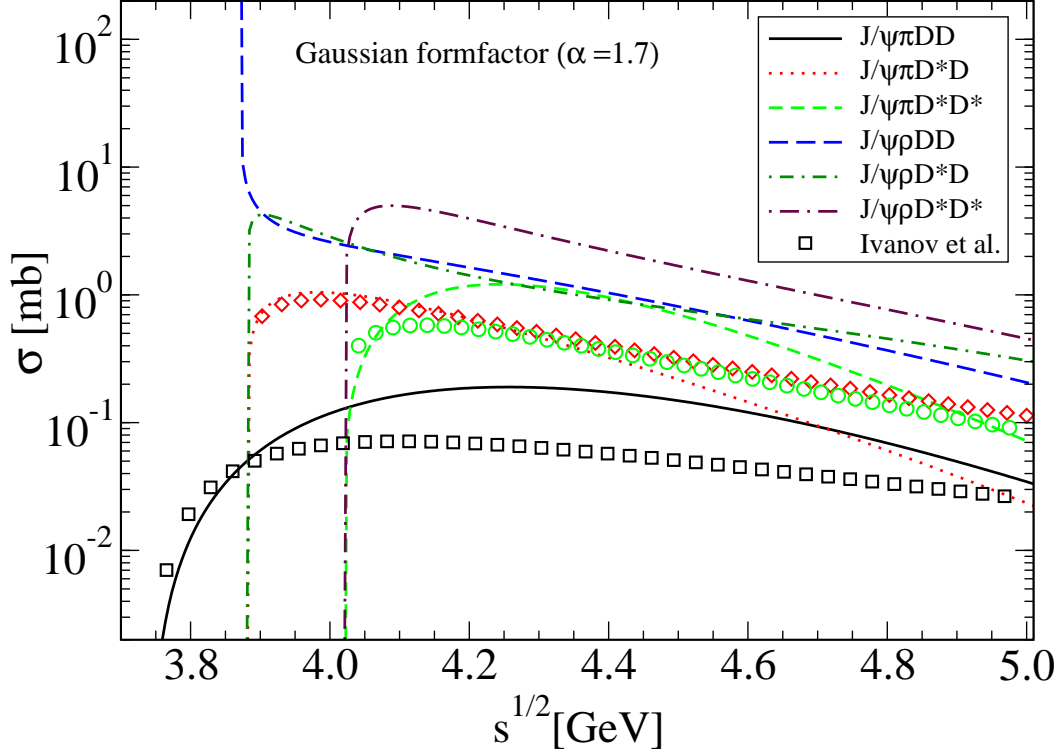


FIG. 4: (Color online)  $J/\psi$  break-up cross sections in the chiral Lagrangian model with Gaussian mesonic formfactors and scale parameter  $\alpha = 1.7$ . Results from the RQM by Ivanov et al. [13] are shown for comparison (symbols).

the corresponding cross sections above the threshold in the sensitive region of the energies  $\sqrt{s} \simeq 4.5$  is about one order of magnitude. This underlines the necessity to improve the hadronic formfactor ansatz and to devise a method of the calibration of the range parameters.

In the left panel Fig. 3 we show the energy dependent cross sections for different processes using the mesonic formfactor model suggested in [21], when the range parameters are chosen as in Table I. In the right panel of the same Figure we vary the parameter  $\alpha$  from 1.0 to 1.7 in order to calibrate this mesonic formfactor model by comparison with the result of Ref. [13] for the process  $J/\psi + \pi \rightarrow D + \bar{D}^*$  dominating at threshold.

Our calculations show that the guess for the range parameters  $\Lambda_i$  successfully reproduces the model calculations of Ref. [13] in the energy range up to  $\sqrt{s} \simeq 4.4$  GeV for values of  $\alpha \simeq 1.7 - 2.2$ , depending on the process considered.

After fixing the parameter  $\alpha = 1.7$  we recalculate the cross sections of all other processes and show the results in Fig. 4. One observes that our calculation gives less suppression than the RQM calculation. These calculations allow us to predict dissociation cross sections also for the  $J/\psi$  dissociation by  $\rho$ -meson impact which are not available in the RQM approach by Ivanov et al. [13]. In comparison to the pion impact processes the  $\rho$  meson processes dominate by a factor 5–8, basically due to the absence or reduction of the reaction threshold.

In order to facilitate phenomenological applications of the energy dependent  $J/\psi$  breakup cross sections obtained in this work, we provide a fit in the form suggested by Barnes et al. in Ref. [25],

$$\sigma(s) = \sigma_{\max} \left( \frac{\varepsilon}{\varepsilon_{\max}} \right)^{p_1} \exp(p_2(1 - \varepsilon/\varepsilon_{\max})) . \quad (15)$$

Here  $\varepsilon = \sqrt{s} - 2M$  denotes the excitation energy above the threshold, where  $M = (m_3 + m_4)/2$  is the mean value of the final state  $D$ -meson masses. In Table II we present the parameter sets obtained from a fit to the  $J/\psi$  breakup cross sections in the MFCL scheme given in Fig. 4. For comparison, the fit parameters corresponding to the RQM results by Ivanov et al. [13] for pion induced reactions are given in brackets. The value  $\varepsilon_{\max}$  corresponds to the excitation energy at which the maximum  $\sigma_{\max}$  of the cross section occurs (if it exists). The parameters  $p_1$  and  $p_2$  characterize the slopes of the rise above threshold and the exponential decay after the maximum, respectively. The latter is a consequence of the fact that at increasing c.m.s. energy the overlap between meson wave functions in momentum space decreases, which determines the amplitude of the quark exchange process (box diagram in the RQM) dominating the result for the cross section. See also Ref. [21] for a discussion of this point.

## V. CONCLUSION

The MFCL scheme developed in the present work removes the ambiguity in the fixation of formfactor parameters by comparison with the RQM approach of Ref. [13] and provides a basis for predicting further  $J/\psi$  absorption cross sections. The first example considered in the present work concerns cross sections for breakup processes by  $\rho$ -meson impact which turn out to be enhanced by one order of magnitude over those resulting from pion impact. This prediction is nicely confirmed by a recent derivation of these cross sections within an extended nonlocal RQM [26]. A future application of the MFCL approach can consider,

process	$\sigma_{\text{max}}[\text{mb}]$	$M[\text{GeV}]$	$\epsilon_{\text{max}}[\text{GeV}]$	$p_1$	$p_2$
$J/\psi\pi DD$	0.1912	1.824	0.6074	3.982	3.982
	(0.07108)	(1.871)	(0.3741)	(1.024)	(1.024)
$J/\psi\pi D^*D$	1.048	1.940	0.1035	0.4925	0.4925
	(0.9105)	(1.937)	(0.1198)	(0.4017)	(0.4017)
$J/\psi\pi D^*D^*$	1.215	2.002	0.2374	1.582	1.582
	(0.5695)	(2.008)	(0.1332)	(0.4774)	(0.4774)
$J/\psi\rho DD$	7.156	1.939	0.00217	-1.804	0.004245
$J/\psi\rho D^*D$	4.234	1.582	0.000162	0.0004756	0.0004756
$J/\psi\rho D^*D^*$	5.068	1.940	0.01891	0.05066	0.05066

TABLE II: Parameters of the cross section fit (15) applied to the results of the MFCL model and those of the RQM by Ivanov et al. [13] (in brackets), corresponding to Fig. 4.

e.g.,  $J/\psi$  dissociation by nucleon impact on the basis of a corresponding chiral Lagrangian calculation [27]. The result of such a work would provide an essential ingredient for the study of  $J/\psi$  suppression in dense nuclear matter as well as for the further analysis of cold nuclear matter effects on  $J/\psi$  production in nuclear collision experiments.

### Acknowledgement

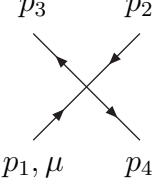
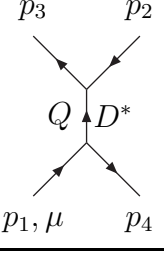
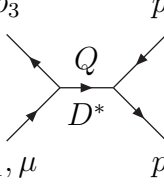
Yu.K. acknowledges support from the Deutsche Forschungsgemeinschaft under grant no. BL 324/3-1, and RFFI no. 06-01-00228. The work of D.B. was supported by the Polish Ministry of Science and Higher Education under grant No. N N 202 0953 33. H.G. was supported in part by the Heisenberg-Landau program of the German Ministry for Education and Research (BMBF).

- 
- [1] M. C. Abreu *et al.* [NA50 Collaboration], Phys. Lett. B **477**, 28 (2000).
  - [2] T. Matsui and H. Satz, Phys. Lett. B **178**, 416 (1986).
  - [3] R. Redmer, Phys. Rep. **282**, 35 (1997).

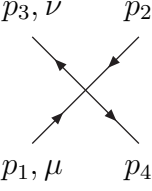
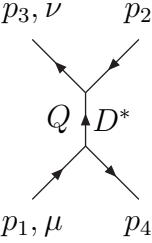
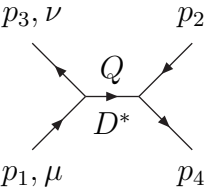
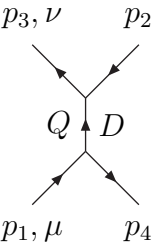
- [4] F. Karsch, M. T. Mehr and H. Satz, Z. Phys. C **37**, 617 (1988).
- [5] G. Röpke, D. Blaschke and H. Schulz, Phys. Lett. B **202**, 479 (1988).
- [6] G. Röpke, D. Blaschke and H. Schulz, Phys. Rev. D **38**, 3589 (1988).
- [7] D. Blaschke, G. Burau, and Y. L. Kalinovsky, “Mott dissociation of D-mesons at the chiral phase transition and anomalous  $J/\psi$  suppression”, in: *Progress in Heavy Quark Physics 5*, Dubna (2000); [arXiv:nucl-th/0006071].
- [8] G. R. G. Burau, D. B. Blaschke, and Y. L. Kalinovsky, Phys. Lett. B **506**, 297 (2001).
- [9] D. Blaschke, G. Burau, Yu. Kalinovsky, V. Yudinchev, Prog. Theor. Phys. Suppl. **149**, 182 (2003).
- [10] K. Martins, D. Blaschke, and E. Quack, Phys. Rev. C **51**, 2723 (1995).
- [11] C. Y. Wong, E. S. Swanson and T. Barnes, Phys. Rev. C **62**, 045201 (2000).
- [12] D. B. Blaschke, G. R. G. Burau, M. A. Ivanov, Yu. L. Kalinovsky and P. C. Tandy, arXiv:hep-ph/0002047.
- [13] M. A. Ivanov, J. G. Körner and P. Santorelli, Phys. Rev. D **70**, 014005 (2004).
- [14] S. G. Matinyan and B. Müller, Phys. Rev. C **58**, 2994 (1998).
- [15] Z. W. Lin and C. M. Ko, Phys. Rev. C **62**, 034903 (2000).
- [16] K. L. Haglin, Phys. Rev. C **61**, 031902 (2000).
- [17] Y. S. Oh, T. Song and S. H. Lee, Phys. Rev. C **63**, 034901 (2001).
- [18] Z. W. Lin, T. G. Di and C. M. Ko, Nucl. Phys. A **689**, 965 (2001).
- [19] K. L. Haglin and C. Gale, Phys. Rev. C **63**, 065201 (2001).
- [20] A. Bourque, C. Gale and K. L. Haglin, Phys. Rev. C **70**, 055203 (2004).
- [21] V. V. Ivanov, Yu. L. Kalinovsky, D. Blaschke and G. R. G. Burau, arXiv:hep-ph/0112354.
- [22] Y. S. Oh, T. S. Song, S. H. Lee and C. Y. Wong, J. Korean Phys. Soc. **43**, 1003 (2003).
- [23] A. Bourque and C. Gale, Phys. Rev. C **78**, 035206 (2008).
- [24] B. Povh and J. Hüfner, Phys. Lett. B **245**, 653 (1990).
- [25] T. Barnes, E. S. Swanson, C. Y. Wong and X. M. Xu, Phys. Rev. C **68**, 014903 (2003).
- [26] A. Bourque and C. Gale, arXiv:0809.3955 [hep-ph].
- [27] W. Liu, C. M. Ko and Z. W. Lin, Phys. Rev. C **65**, 015203 (2002).

## APPENDIX A: DIAGRAMS, AMPLITUDES AND COUPLINGS

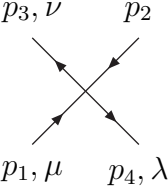
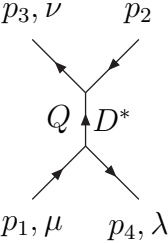
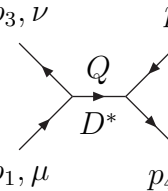
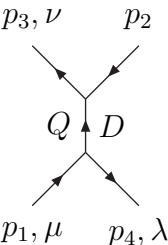
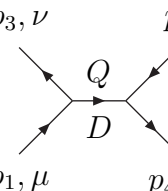
### 1. The process: $J/\psi(p_1, \mu) + \pi(p_2) \longrightarrow D(p_3) + \bar{D}(p_4)$

Diagram	Amplitude	Coupling
	$M_\mu^{(1)} = A_1 \epsilon_{\mu\nu\alpha\beta} p_2^\nu p_3^\alpha p_4^\beta$	$A_1 = g_{J/\psi\pi D\bar{D}}$
	$M_\mu^{(2)} = A_2 \epsilon_{\mu\nu\alpha\beta} p_1^\nu p_4^\alpha (p_2)_\sigma N_{D^*}^{\sigma\beta}(Q)$	$A_2 = -\frac{g_{J/\psi D^* \bar{D}} g_{D^* D \pi}}{u - m_{D^*}^2}$
	$M_\mu^{(3)} = A_3 \epsilon_{\mu\nu\alpha\beta} p_1^\nu p_3^\alpha (p_2)_\sigma N_{D^*}^{\sigma\beta}(Q)$	$A_3 = -\frac{g_{J/\psi D^* \bar{D}} g_{D^* D \pi}}{t - m_{D^*}^2}$

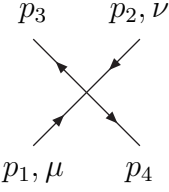
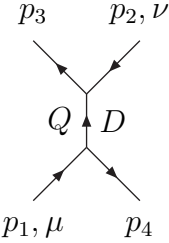
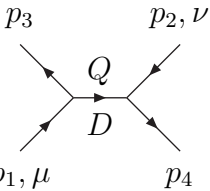
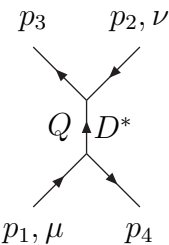
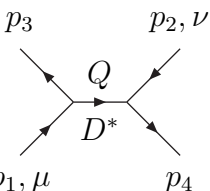
**2. The processes:**  $J/\psi(p_1, \mu) + \pi(p_2) \longrightarrow D^*(p_3, \nu) + \bar{D}(p_4), D(p_3) + \bar{D}^*(p_4, \nu)$

Diagram	Amplitude	Coupling
	$M_{\mu\nu}^{(1)} = C_1 g_{\mu\nu}$	$C_1 = g_{J/\psi\pi D\bar{D}^*}$
	$M_{\mu\nu}^{(2)} = C_2 \epsilon_{\mu\gamma\delta\beta} \epsilon_{\nu\lambda\rho\alpha} p_1^\gamma p_4^\delta p_3^\lambda p_2^\rho N_{D^*}^{\alpha\beta}(Q)$	$C_2 = -\frac{g_{J/\psi D^* \bar{D}} g_{D^* D^* \pi}}{u - m_{D^*}^2}$
	$M_{\mu\nu}^{(3)} = C_3 [2g_{\alpha\nu}(p_3)_\mu - g_{\mu\nu}(p_1 + p_3)_\alpha + 2g_{\alpha\mu}(p_1)_\nu] N_{D^*}^{\alpha\beta}(Q)(p_2 + p_4)_\beta$	$C_3 = \frac{g_{J/\psi D^* \bar{D}} g_{D^* D \pi}}{t - m_{D^*}^2}$
	$M_{\mu\nu}^{(4)} = C_4 4 (p_2)_\nu (p_4)_\mu$	$C_4 = -\frac{g_{J/\psi D \bar{D}} g_{D^* D \pi}}{u - m_D^2}$

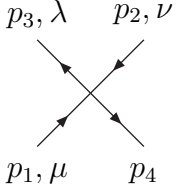
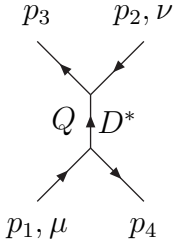
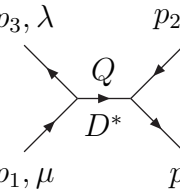
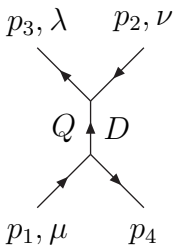
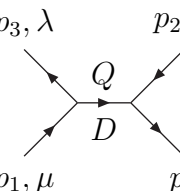
**3. The process:**  $J/\psi(p_1, \mu) + \pi(p_2) \longrightarrow D^*(p_3, \nu) + \bar{D}^*(p_4, \lambda)$

Diagram	Amplitude	Coupling
	$M_{\mu\nu\lambda}^{(1)} = B_{11}\epsilon_{\mu\nu\lambda\beta}p_2^\beta + B_{12}\epsilon_{\mu\nu\lambda\beta}p_1^\beta$	$B_{11} = g_{J/\psi\pi D^*\bar{D}^*}$ $B_{12} = g_{J/\psi\pi D^*\bar{D}^*}$
	$M_{\mu\nu\lambda}^{(2)} = B_2\epsilon_{\nu\gamma\delta\alpha}[2g_{\mu\beta}(p_1)_\lambda - g_{\mu\lambda}(p_1 + p_4)_\beta + 2g_{\lambda\beta}(p_4)_\mu]$ $N_{D^*}^{\alpha\beta}(Q)p_3^\gamma p_2^\delta$	$B_2 = \frac{g_{J/\psi D^*\bar{D}^*} g_{D^* D^* \pi}}{u - m_{D^*}^2}$
	$M_{\mu\nu\lambda}^{(3)} = B_3\epsilon_{\lambda\gamma\delta\alpha}[2g_{\nu\beta}(p_3)_\mu - g_{\mu\nu}(p_1 + p_3)_\beta + 2g_{\mu\beta}(p_1)_\nu]$ $N_{D^*}^{\alpha\beta}(Q)p_2^\gamma p_4^\delta$	$B_3 = \frac{g_{J/\psi D^*\bar{D}^*} g_{D^* D^* \pi}}{t - m_{D^*}^2}$
	$M_{\mu\nu\lambda}^{(4)} = B_4\epsilon_{\mu\lambda\alpha\beta}p_1^\alpha p_4^\beta (p_2)_\nu$	$B_4 = -\frac{2g_{J/\psi D^*\bar{D}} g_{D^* D \pi}}{u - m_D^2}$
	$M_{\mu\nu\lambda}^{(5)} = B_5\epsilon_{\mu\nu\alpha\beta}p_1^\alpha p_3^\beta (p_2)_\lambda$	$B_5 = \frac{2g_{J/\psi D^*\bar{D}} g_{D^* D \pi}}{t - m_D^2}$

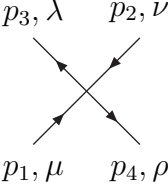
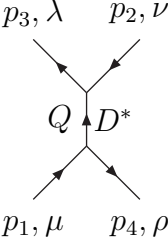
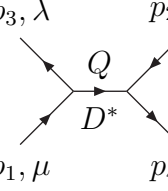
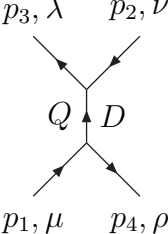
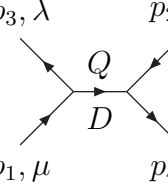
4. **The process:**  $J/\psi(p_{1,\mu}) + \rho(p_{2,\nu}) \longrightarrow D(p_3) + \bar{D}(p_4)$

Diagram	Amplitude	Coupling
	$M_{\mu\nu}^{(1)} = G_1 \delta_{\mu\nu}$	$G_1 = g_{J/\psi \rho D \bar{D}}$
	$M_{\mu\nu}^{(2)} = G_2 4(p_3)_\nu (p_4)_\mu$	$G_2 = \frac{g_{J/\psi D \bar{D}} g_{D D \rho}}{u - m_D^2}$
	$M_{\mu\nu}^{(3)} = G_3 4(p_3)_\mu (p_4)_\nu$	$G_3 = \frac{g_{J/\psi D \bar{D}} g_{D D \rho}}{t - m_D^2}$
	$M_{\mu\nu}^{(4)} = G_4 \epsilon_{\nu \rho \sigma \alpha} \epsilon_{\mu \lambda \gamma \beta} p_1^\lambda p_2^\sigma p_3^\rho p_4^\gamma N_{D^*}^{\alpha\beta}(Q)$	$G_4 = \frac{g_{J/\psi D \bar{D}^*} g_{D^* D \rho}}{u - m_{D^*}^2}$
	$M_{\mu\nu}^{(5)} = G_5 \epsilon_{\nu \rho \sigma \alpha} \epsilon_{\mu \lambda \gamma \beta} p_1^\lambda p_2^\sigma p_3^\gamma p_4^\rho N_{D^*}^{\alpha\beta}(Q)$	$G_5 = \frac{g_{J/\psi D \bar{D}^*} g_{D^* D \rho}}{t - m_{D^*}^2}$

**5. The process:**  $J/\psi(p_1, \mu) + \rho(p_2, \nu) \longrightarrow D^*(p_3, \lambda) + \bar{D}(p_4), D(p_3) + \bar{D}^*(p_4, \lambda)$

Diagram	Amplitude	Coupling
	$M_{\mu\nu\lambda}^{(1)} = H_{11}\epsilon_{\mu\nu\lambda\beta}p_3^\beta + H_{12}\epsilon_{\mu\nu\lambda\beta}p_4^\beta$	$H_{11} = g_{J/\psi\rho D^*D}$ $H_{12} = g_{J/\psi\rho DD^*}$
	$M_{\mu\nu\lambda}^{(2)} = H_2\epsilon_{\mu\rho\sigma\alpha} [2g_{\lambda\beta}(p_3)_\nu - g_{\lambda\nu}(p_2 + p_3)_\beta + 2(p_2)_\lambda g_{\nu\beta}]$ $N_{D^*}^{\alpha\beta}(Q)p_1^\rho p_4^\sigma$	$H_2 = \frac{g_{\rho D^* \bar{D}^*} g_{J/\psi D^* D}}{u - m_{D^*}^2}$
	$M_{\mu\nu\lambda}^{(3)} = H_3\epsilon_{\nu\rho\sigma\alpha} [2g_{\lambda\beta}(p_3)_\mu - g_{\lambda\mu}(p_1 + p_3)_\beta + 2g_{\mu\beta}(p_1)_\lambda]$ $N_{D^*}^{\alpha\beta}(Q)p_2^\rho p_4^\sigma$	$H_3 = -\frac{g_{J/\psi D^* \bar{D}^*} g_{\rho D^* D}}{t - m_{D^*}^2}$
	$M_{\mu\nu\lambda}^{(4)} = H_4\epsilon_{\nu\lambda\alpha\beta}p_2^\alpha p_3^\beta (p_4)_\mu$	$H_4 = -\frac{2g_{J/\psi D \bar{D}} g_{\rho D^* D}}{u - m_D^2}$
	$M_{\mu\nu\lambda}^{(5)} = H_5\epsilon_{\mu\lambda\alpha\beta}p_1^\alpha p_3^\beta (p_4)_\nu$	$H_5 = \frac{2g_{J/\psi D^* \bar{D}} g_{\rho DD}}{t - m_D^2}$

**6. The processes:**  $J/\psi(p_1, \mu) + \rho(p_2, \nu) \longrightarrow D^*(p_3, \lambda) + \bar{D}^*(p_4, \rho)$

Diagram	Amplitude	Coupling
	$M_{\mu\nu\lambda\rho}^{(1)} = K_1 [2g_{\mu\nu}g_{\rho\lambda} - g_{\mu\rho}g_{\nu\lambda} - g_{\mu\lambda}g_{\nu\rho}]$	$K_1 = g_{J/\psi\rho D^*\bar{D}^*}$
	$M_{\mu\nu\lambda\rho}^{(2)} = K_2 [2g_{\rho\alpha}(p_4)_\mu - g_{\mu\rho}(p_1 + p_4)_\alpha + 2g_{\mu\alpha}(p_1)_\rho]$ $N_{D^*}^{\alpha\beta}(Q)$ $[2g_{\beta\lambda}(p_3)_\nu - g_{\nu\lambda}(p_2 + p_3)_\beta + 2g_{\beta\nu}(p_2)_\lambda]$	$K_2 = \frac{g_{J/\psi D^*\bar{D}^*} g_{\rho D^* D^*}}{u - m_{D^*}^2}$
	$M_{\mu\nu\lambda\rho}^{(3)} = K_3 [2g_{\lambda\alpha}(p_3)_\mu - (p_1 + p_3)_\alpha g_{\mu\lambda} + 2g_{\mu\alpha}p_1^\lambda]$ $N_{D^*}^{\alpha\beta}(Q)$ $[2g_{\beta\rho}(p_4)_\nu - g_{\nu\rho}(p_2 + p_4)_\beta + 2g_{\beta\nu}(p_2)_\rho]$	$K_3 = \frac{g_{J/\psi D^*\bar{D}^*} g_{\rho D^* D^*}}{t - m_{D^*}^2}$
	$M_{\mu\nu\lambda\rho}^{(4)} = K_4 \epsilon_{\mu\rho\alpha\beta} \epsilon_{\nu\lambda\gamma\delta} p_1^\alpha p_2^\gamma p_3^\beta p_4^\delta$	$K_4 = \frac{g_{J/\psi D^*\bar{D}} g_{\rho D^* D}}{u - m_D^2}$
	$M_{\mu\nu\lambda\rho}^{(5)} = K_5 \epsilon_{\mu\lambda\alpha\beta} \epsilon_{\nu\rho\gamma\delta} p_1^\alpha p_2^\gamma p_3^\beta p_4^\delta$	$K_5 = \frac{g_{J/\psi D^*\bar{D}} g_{\rho D^* D}}{t - m_D^2}$

**APPENDIX B: COUPLING CONSTANTS**

Here we summarize the values of the coupling constants occuring in the amplitudes of the Appendix A. They correspond to those given in Ref. [17]

Coupling constants	Value
$g_{J/\psi\pi DD}$	16.0 GeV <sup>-3</sup>
$g_{J/\psi\pi DD^*}$	33.92
$g_{J/\psi\pi D^*D^*}$	38.19 GeV <sup>-1</sup>
$g_{J/\psi\rho DD}$	38.86
$g_{J/\psi\rho DD^*}$	21.77 GeV <sup>-1</sup>
$g_{J/\psi\rho D^*D^*}$	19.43
$g_{J/\psi DD}$	7.71
$g_{J/\psi D^*D}$	8.64 GeV <sup>-1</sup>
$g_{J/\psi D^*D^*}$	7.71
$g_{D^*D\pi}$	8.84
$g_{D^*D^*\pi}$	9.08 GeV <sup>-1</sup>
$g_{DD\rho}$	2.52
$g_{D^*D\rho}$	2.82 GeV <sup>-1</sup>
$g_{D^*D^*\rho}$	2.52

TABLE III: Values for the coupling constants introduced in the amplitudes for the processes given in Appendix A.